The biological characteristics and infection dynamics of a novel H3N2 canine influenza virus genotype in beagles

Fei-fei Ge[1†], Hai-xiao Shen[1†], De-quan Yang[1], Xian-chao Yang[1], Xin Li[1], Jian Wang[1*] and Shixin Huang[1*]

Abstract

Background The canine influenza virus (CIV) outbreak has garnered considerable attention as it poses a significant threat to dog health. During the H3N2 CIV evolution in beagles, the virus formed a new clade after 2019 and gradually became more adaptable to other mammals. Therefore, successfully elucidating the biological characteristics and constructing a canine influenza infection model is required for CIV characterization.

Methods We performed genetic analyses to examine the biological characteristics and infection dynamics of CIV.

Results The genotype of our H3N2 CIV strain (from 2019 in Shanghai) belonged to the 5.1 clade, which is now prevalent in China. Using MDCK cells, we investigated viral cytopathic effects. Virus size and morphology were observed using transmission electron microscopy. Beagles were also infected with 10^4, 10^5, and 10^6 50% egg-infectious doses (EID_{50}). When compared with the other groups, the 10^6 EID_{50} group showed the most obvious clinical symptoms, the highest virus titers, and typical lung pathological changes. Our results suggested that the other two treatments caused mild clinical manifestations and pathological changes. Subsequently, CIV distribution in the 10^6 EID_{50} group was detected by hematoxylin and eosin (H&E) and immunofluorescence (IF) staining, which indicated that CIV primarily infected the lungs.

Conclusions The framework established in this study will guide further CIV prevention strategies.

Keywords Canine influenza virus, 5.1 clade, Biological characteristics, Infection dynamics, Beagles

[†]Fei-Fei Ge and Hai-xiao Shen contributed equally to this work as co-first authors

*Correspondence:
Jian Wang
jianwhlj@163.com
Shixin Huang
huangshx1968@sina.com
[1]Shanghai Animal Disease Control Center, Shanghai 201103, People's Republic of China

Background

Canine influenza virus (CIV) belongs to the Orthomyxoviridae family and contains eight single-stranded negative RNA fragments encoding more than 15 viral proteins [1]. Dogs are susceptible to avian influenza virus (H3N2 and H5N1), equine influenza virus (H3N8), or human influenza virus (pdmH1N1 and H3N2) [2–4]. Globally, H3N8 and H3N2 are the major CIV subtypes [4]. H3N8 CIV has been circulating mainly in the United States since 2004 [5], while H3N2 CIV is dominant in South Korea and China [4, 6]. When compared with H3N8 CIV, H3N2 CIV has a wider host range and infects various mammals, including ferrets, guinea pigs, mice, and cats [7–10].

Ge *et al. Virology Journal* (2024) 21:151

Page 2 of 8

Throughout history, influenza pandemics have been caused by the introduction of new viruses. Pigs are a "mixed container" of influenza A virus (IAV) in birds and mammals, while dogs are the most likely animals to come into contact with humans, and are suspected as potential mixed containers. As one of the most popular pets, dogs have close contact with humans, so CIV spread poses a serious threat to the human influenza virus. However, studies on animals infected with CIV have been conducted. H3N2 CIV pathogenesis is contradictory. Research has shown that H3N2 CIV damages organs and the respiratory tract, with virus titers detected in corresponding tissues [11]. In contrast, low pathogenic H3N2 CIV and even highly pathogenic H5N1 CIV are the main causes of damage to the tonsils and respiratory tract, with virus titers undetected in other organs [12–14]. These results indicate that CIV clinical symptoms and virus replication dynamics are highly dependent on individual differences in the infection strain, the vaccination route, and host immunity [15–18]. Therefore, the comprehensive confirmation of H3N2 CIV pathogenicity in dogs is required. In our study, a new CIV genotype was cultured in MDCK cells supplemented with 2% Dulbecco's Modified Eagle Medium and trypsin, treated with 1 μg/ml TPCK, and observed under electron microscopy. We also investigated viral infection dynamics in beagles.

Methods

Ethics statement
Animal protocols were approved by the Laboratory Animals Ethics Committee of the Shanghai Animal Disease Control Center.

Phylogenetic analyses
The hemagglutinin (*HA*) genes of six H3N2 CIV isolates (A/canine/China/Shanghai/0103/2019; A/canine/China/Shanghai/0104/2019; A/canine/China/Shanghai/0105/2019; A/canine/China/Shanghai/018/2019; A/canine/China/Shanghai/019/2019; A/canine/China/Shanghai/0114/2019) from Shanghai in 2019 were used for genetic and phylogenetic analyses (Accession numbers; MK758007.1–MK7580054.1). Sequence data were compiled and edited using Lasergene sequence analysis software (Dnastar Inc., Madison, WI, USA). Multiple sequence alignments were conducted using CLUSTAL W. The maximum likelihood tree for origin analysis was constructed in MEGA 4 using 1,000 bootstrap replications [19, 20].

Virus propagation and electron microscopy
A/canine/Shanghai/0103/2019 (H3N2) was isolated from a stray dog in Shanghai, China. The virus was propagated in 9 day old specific pathogen-free (SPF) embryonated chicken eggs at 37 °C for 48 h and stored at -80 °C.

Viral titers were evaluated using the 50% egg-infectious dose (EID_{50}/ml) method and calculated using the Reed–Muench method [21]. For virus isolation using MDCK cells, 1 μg/ml TPCK-treated trypsin was used to support viral growth. Infected cells were incubated under 5% CO_2 at 37 °C for 72 h. Supernatants were harvested and further passaged. Then, infection was detected using RT-PCR (Qiagen, Shenzhen). The H3N2 virus (A/canine/Shanghai/0103/2019) was adsorbed onto a carbon parlodion-coated copper grid for 2 min. Excess suspension was removed by blotting with filter paper, and the grid was immediately stained with 1% phosphotungstic acid for 10 min. Excess stain was removed using filter paper, after which samples were examined using a transmission electron microscope (Hitachi, Japan).

Clinical studies and viral challenge
Sixteen beagles (10 weeks old) were obtained from the Experimental Animal Center (Runde Biotechnology Co., Ltd., Shanghai, China). Prior to studies, serum samples were collected from all dogs and subjected to hemagglutination inhibition (HI) assays to ensure that animals had not been exposed to H3N2 CIV. Four dogs were used as controls. For intranasal administration, the 12 remaining dogs were divided into three groups and intranasally inoculated with 1 ml of 10^4, 10^5, or 10^6 EID_{50} of A/canine/Shanghai/0103/2019. The control group was intranasally inoculated with the same volume of sterile phosphate-buffered saline (PBS). Dogs were housed in separate cages and observed for 10 days after infection.

Nasal swabs were collected, during which time clinical symptoms were monitored. The clinical score of each dog was evaluated using a previously described scoring system [22]. Nasal secretions were collected from left and right nostrils every day until day 10 after inoculation (0–10 days post infection (dpi)) and diluted in 1 ml of PBS plus 1% penicillin and streptomycin. Nasal swabs were used for measuring EID_{50} values using 9–11 day old embryonic chicken eggs. Two dogs from the control group and two from each experimental group were then humanely euthanized at 5 dpi. Turbinates, tracheas, and lung tissues were collected, and EID_{50} sample values determined. Briefly, 1 ml of sterile PBS was added per 1 g of collected tissue, which was then ground in a liquid nitrogen homogenizer. Supernatants were collected by centrifugation and inoculated at different dilutions into 9 day old chicken embryos. The two remaining dogs in groups were monitored until day 10.

Serological testing
Blood samples were collected from dogs at 2, 4, 6, 8, and 10 dpi. Approximately 500 μl of serum was collected from each dog and stored at -20 °C until required. One volume of serum was mixed with three volumes of

receptor-destroying enzyme (RDE, Denka Seiken Co., Ltd.), incubated for 18 h at 37 ℃ and then 30 min at 56 ℃. Antiserum titers were determined using HI assays. The 1% red blood cells used in this study were collected from SPF cocks and diluted in sterile PBS.

Histopathological examinations using hematoxylin & eosin (H&E) and immunofluorescence (IF) staining

Liver, spleen, lung, trachea, and intestinal tissues collected at 5 dpi were fixed in 10% formalin for >48 h. Samples were washed overnight, dehydrated in alcohol, and embedded in paraffin. Next, paraffin-embedded tissues were cut into 4–7 µm thick sections and deposited on glass slides. Sections were then mounted and left overnight at 37 ℃ prior to H&E staining.

IF staining was performed on deparaffinized and rehydrated tissue sections. Briefly, sections were first treated with antigen unmasking solution (Vector Laboratories, California, USA) in a pressure cooker. After blocking in 0.1% Sudan black B for 15 min and 1% bovine serum albumin/PBS at room temperature for 30 min, membranes were incubated with a primary antibody against IAV nucleoprotein (Abcam) at 4 ℃ overnight. This

was followed by incubation with Cy5-conjugated goat anti-mouse IgG (Abcam) for 30 min, after which sections were stained with 4′,6-diamidino-2-phenylindole (Thermo Fisher Scientific). All sections were examined and images captured using a Carl Zeiss LSM780 confocal microscope.

Statistical analyses

Statistical significance was determined using one-way analysis of variance with *post hoc* Tukey's multiple-comparison tests using GraphPad Prism (v.7.02) software (GraphPad Software, Inc., La Jolla, CA, USA). P values < 0.05 indicated statistical significance.

Results

Phylogenetic analysis

To better characterize genetic variations in the six isolated H3N2 CIVs from Shanghai, the *HA* segment of all six H3N2 CIVs were analyzed and fell into clade 5.1, which is prevalent in China (Fig. 1). Our six isolates belonged to the same clade as the reference strains [23].
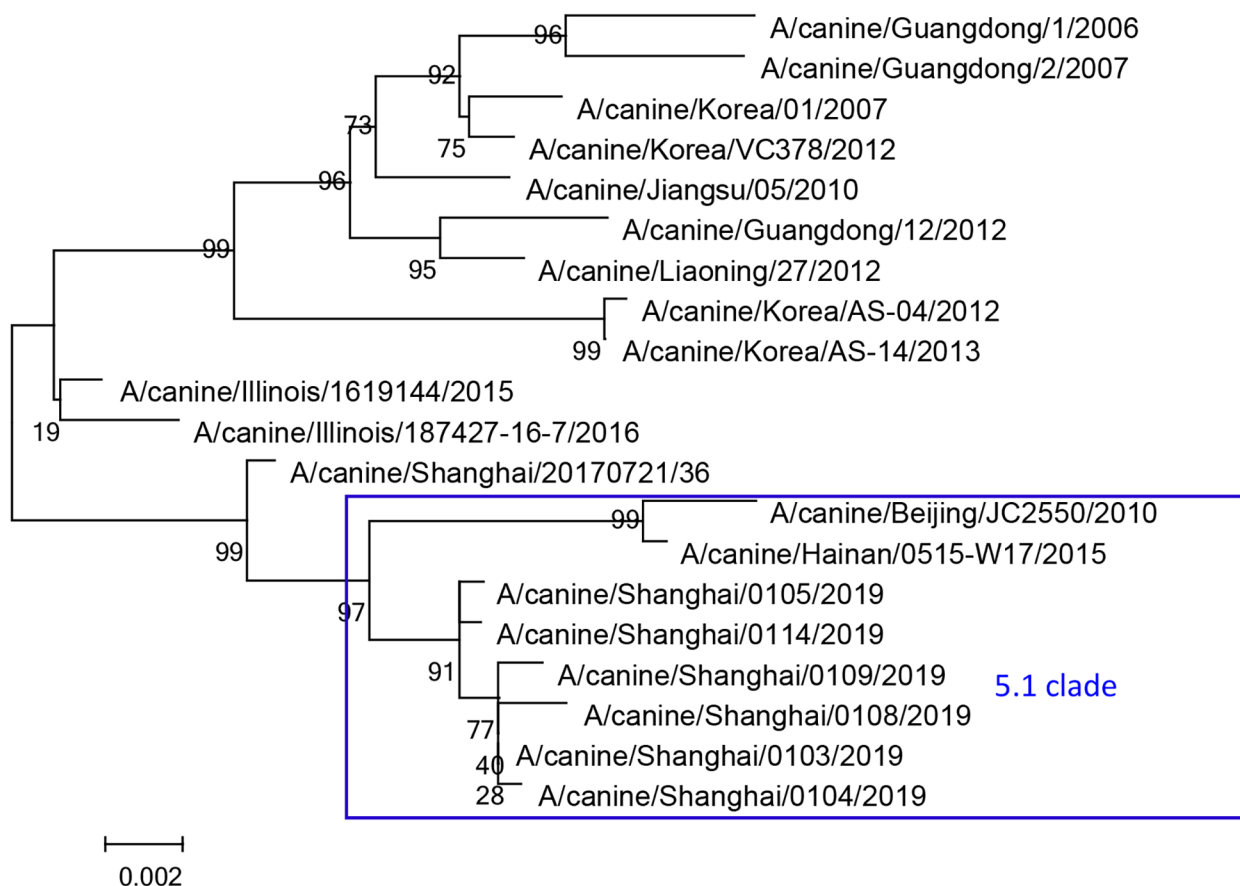
Fig. 1 A phylogenetic tree showing the hemagglutinin segment of H3N2 CIVs. The 2019 isolates included in this study are highlighted in the blue square

Virus propagation and electron microscopy

To further investigate viral biological characteristics, MDCK cells were used. The isolate showed remarkable cytopathic effects toward MDCK cells (Fig. 2A and B). H3N2 CIV was detected using RT-PCR (Qiagen, Shenzhen) (Fig. 2C). Virus size and morphology were both examined using transmission electron microscopy; the average size was 100 nm, and spikes were observed on spherical surfaces (Fig. 3).

Clinical symptoms

Different CIV dose replication and pathogenicity outcomes were systematically compared in beagles. All challenged dogs showed respiratory symptoms at 2 dpi,
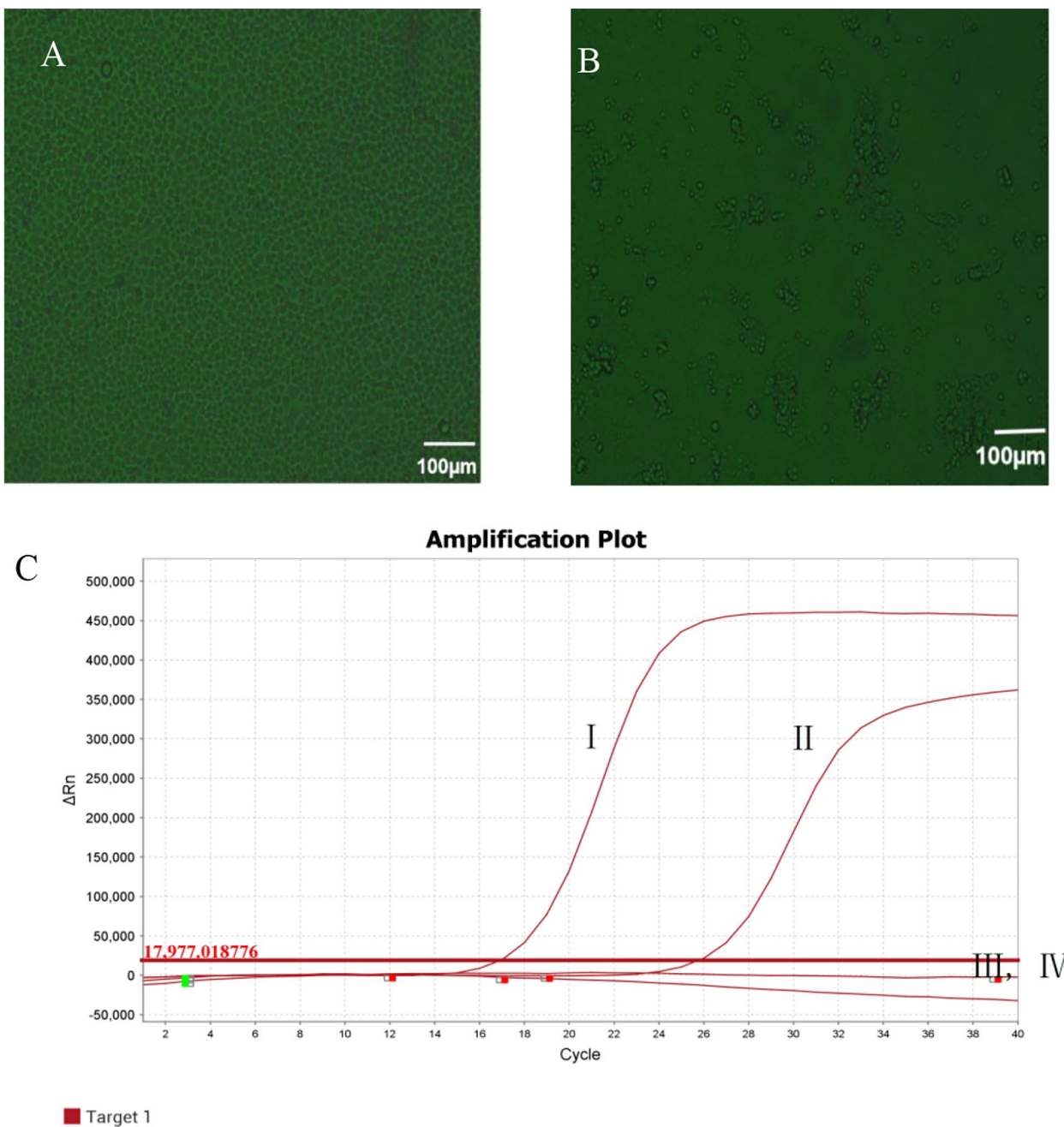
Fig. 2 CIV cytopathic effects on MDCK cells at 36 h post-inoculation (hpi) (100× magnification). **(A)** Mock-inoculated MDCK cell culture (normal cells). **(B)** A/Canine/Shanghai/0103/2019-inoculated MDCK cells showing rounded and clustered cells. **(C)** Amplification Plots I: A/Canine/ Shanghai/0103/2019-inoculated MDCK cells; II: Positive control; III: Mock-inoculated MDCK cells; and IV: Negative control
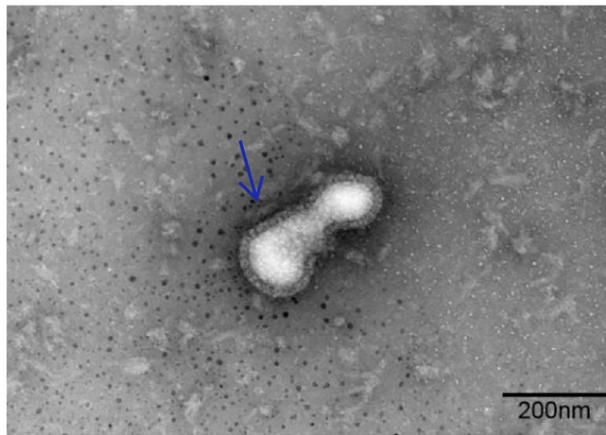
Fig. 3 Negative electron microscopy staining of H3N2 CIV (A/canine/Shanghai/0103/2019) (blue arrow)

including sneezing, nose clearing, depression, and coughing, which continued until day 8 (Fig. 4A, B).

When the infectious dose was 10^6 EID_{50}, clinical symptom scores were greater than the other two experimental groups at 4 and 6 dpi. The difference between the 10^6 EID_{50} group and the other groups was significant at 6 dpi ($P<0.05$) (Fig. 5A). When compared with the control group, body temperatures in infected dogs fluctuated to varying degrees, and fever always occurred at 2–6 dpi (Fig. 5B).

The virus was detected within 24 h post-inoculation, and virus shedding lasted for 1–6 days in all challenged dogs. The virus titer in the 10^6 EID_{50} group was significantly greater than in the other two groups at 1–5 dpi ($P<0.05$). No virus was detected on the 7th day, showing that virus shedding terminated at 7 dpi in beagles (Fig. 5C). As shown (Fig. 5D), virus titers were evaluated in turbinates, tracheas, and lungs in infected dogs at 5 dpi. In turbinates and lungs, but not in tracheas, virus

titers in 10^6 EID_{50} and 10^5 EID_{50} groups were significantly greater than titers in the 10^4 EID_{50} group ($P<0.05$).

Seroconversion (HI titers)
To determine antibody responses to CIV-H3N2, challenged dogs were analyzed and were seropositive at 6–10 dpi. At 6 dpi, serum antibody levels in all challenged groups were increased. When compared with 10^4 EID50 group levels, 10^5 EID_{50} and 10^6 EID_{50} group levels were significantly higher at 8 dpi ($P<0.05$) (Fig. 6).

Anatomical examinations
Influenza can cause acute lung injury. An anatomical lung examination revealed that 10^6 EID_{50} and 10^5 EID_{50} groups showed obvious lesions; lung surfaces had visible bleeding spots. However, visible lesions were barely detected in 10^4 EID_{50} group lungs (Fig. 7A–D).

H&E and IF staining
To identify virus-infected tissues, at 5 dpi, liver, spleen, lung, trachea, and intestinal tissues were collected from the 10^6 EID50 group for H&E and IF staining. Lung pathological lesions, including interstitial pneumonia and hepatocyte degeneration and swelling, were observed (Fig. 8A). As shown (Fig. 8B), strong CIV antigen staining was observed in lungs, while no CIV antigen staining was detected in the liver (Fig. 8).

Discussion
As a popular companion, dogs typically have close contact with humans and are considered potential intermediate IAV hosts [24]. Canine influenza has occurred in Shanghai and other places in recent years, and potentially threatens public health safety. Research on H3N2 subtype CIV pathogenicity can help us better understand disease pathogenesis, vaccine research and evaluation. Therefore, six H3N2 CIV strains from Shanghai were
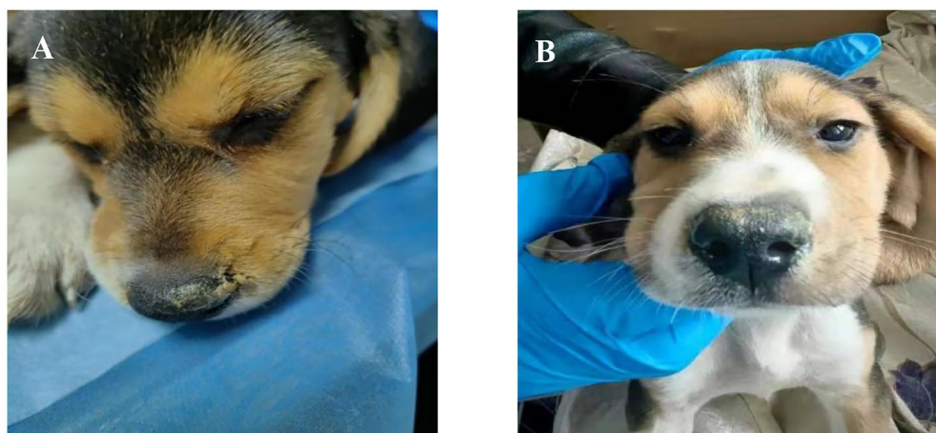
**Fig. 4** Infected dogs show depression (**A**) and a streaming nose (**B**) at 2 dpi
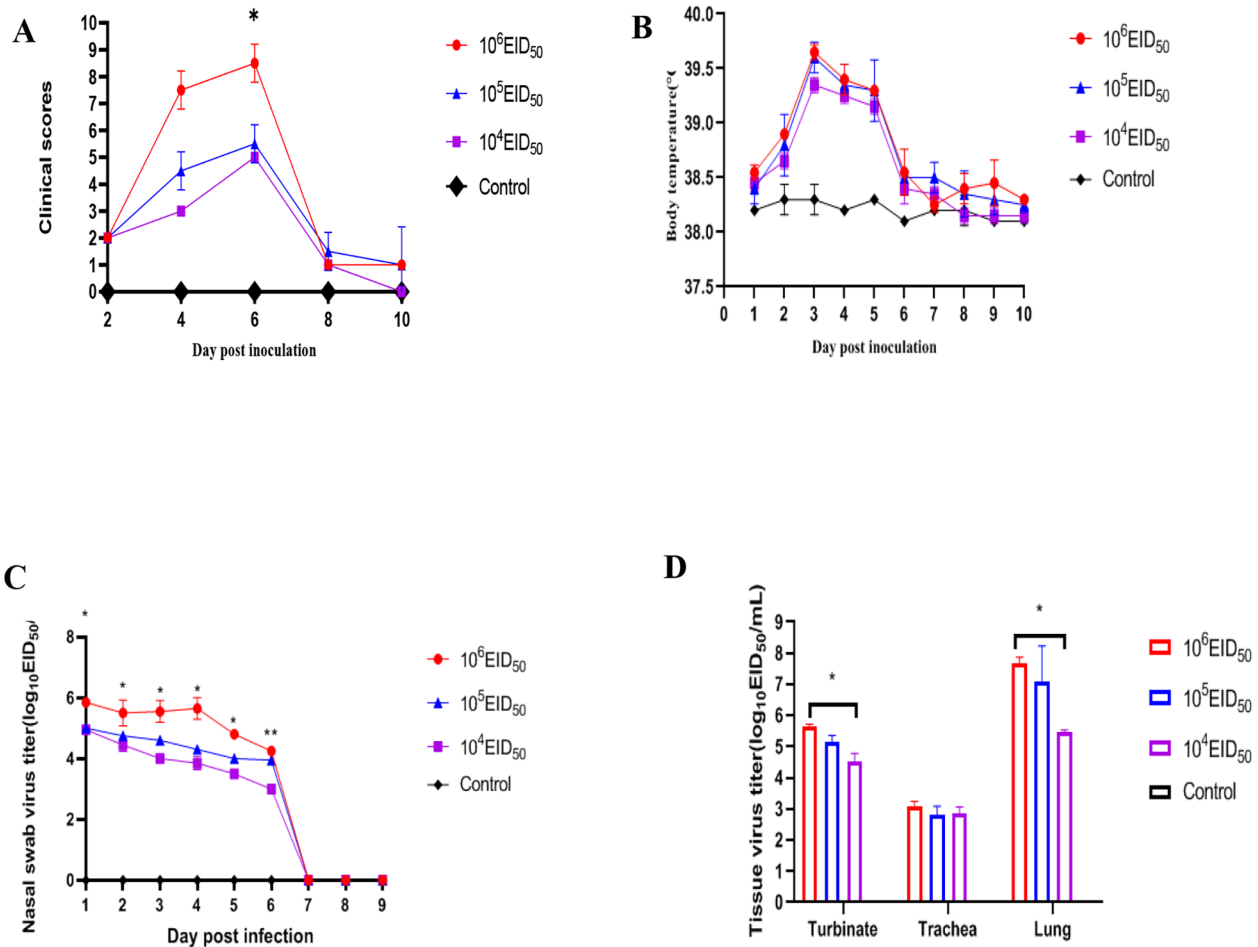
Fig. 5 Dogs were inoculated with 10^6, 10^5, or 10^4 EID$_{50}$ ($n=2$) of the A/canine/Shanghai/0103/2019 virus or PBS ($n=2$) as a control. Nasal turbinate, trachea, and lung tissues were collected after humanely euthanizing two dogs in each group at 5 dpi. **(A)** After infection with H3N2 CIV at days 2, 4, 6, 8, and 10, clinical scores were recorded; **(B)** Body temperatures were recorded at 1–10 dpi; **(C)** Nasal swabs were evaluated by EID$_{50}$ assays at 1–9 dpi (note: no significant difference between 10^6 EID$_{50}$ and 10^5 EID$_{50}$ groups at 6 dpi were recorded; a significant difference was recorded between 10^6 EID$_{50}$, 10^5 EID$_{50}$, and 10^4 EID$_{50}$ groups at 6 dpi). **(D)** Tissue virus titer. EID$_{50}$ assays were conducted to evaluate virus titers in turbinates, tracheas, and lung tissues at 5 dpi (*$P < 0.05$)
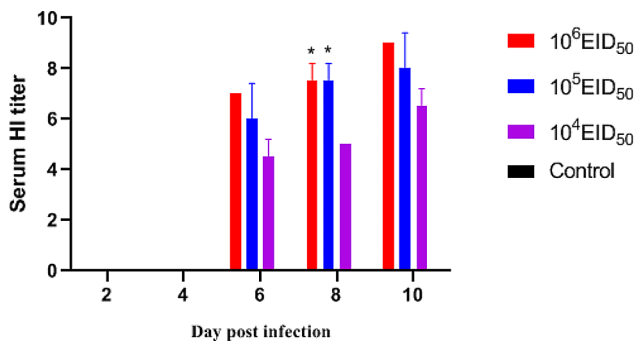

Fig. 6 Hemagglutination inhibition (HI) titers showing serum-specific antibody levels ($n=2$) (*$P < 0.05$)

analyzed according to the report by Chen et al.; these strains belonged to the 5.1 clade, which is now prevalent in China [23]. We also confirmed that H3N2 subtype CIV caused high fever, shortness of breath, cough, and severe lung consolidation in dogs, largely consistent with published H3N2 CIV pathogenicity [25, 26]. To prevent further CIV, infection dynamics in beagle were investigated. We compared clinical scores, body temperatures, nasal swab wash virus titers, tissue virus titers, and lung tissue damage between different titer groups (10^4 EID$_{50}$, 10^5 EID$_{50}$, and 10^6 EID$_{50}$). Overall, when compared with other lower intranasal doses, the intranasal 10^6 EID$_{50}$ dose caused obvious clinical symptoms and tissue damage. At 6 dpi, more than 2^4 HI titers were induced in challenged groups. The body induces immune responses
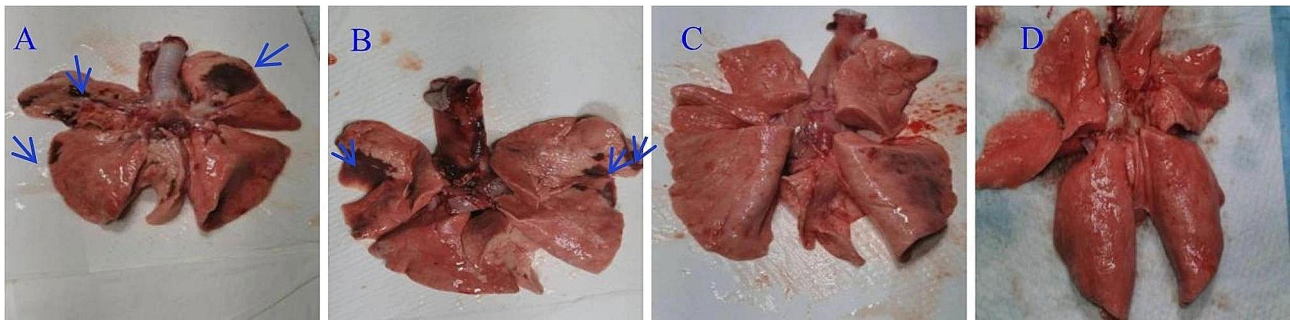
Fig. 7 Macroscopic images showing beagle lungs. **(A)** 10^6 EID_{50}; **(B)** 10^5 EID_{50}; **(C)** and 10^4 EID_{50} challenge groups, **(D)** normal beagle lungs. The blue arrows indicate tissue damage
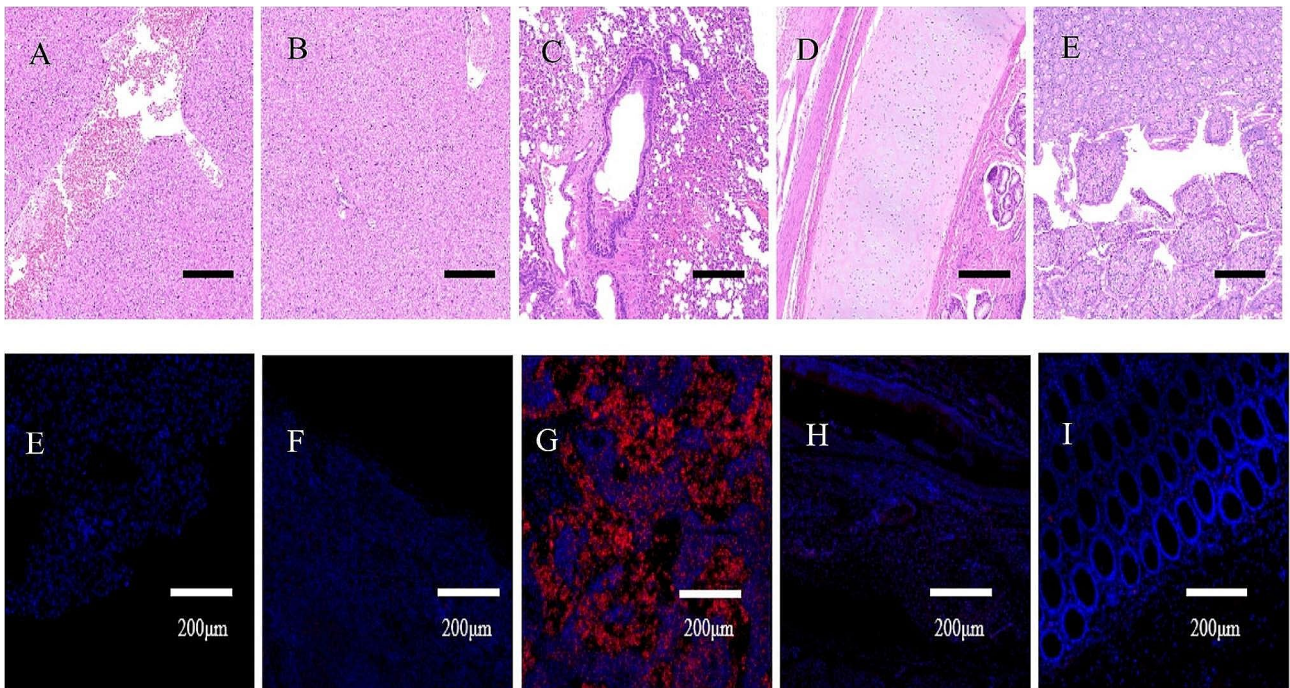
Fig. 8 At 5 dpi, liver, spleen, lung, trachea, and intestinal tissues were collected for hematoxylin and eosin **(A–D)** and immunofluorescence staining **(E–H)**

against IAVs, which often cause secondary bacterial diseases and lung diseases after infection [27].

Influenza virus mainly infects the upper respiratory tract and bronchial epithelial cells, but in severe cases, it can spread to the bronchioles and alveoli to cause interstitial pneumonia. To assess the degree of lung injury caused by different challenges, we collected lung tissues from infected beagles at 5 dpi. With increasing dose, clinical symptoms in dogs were more obvious; lung lesions were more serious, and the attack dose positively correlated with disease severity. Furthermore, we tested the tissue tropism of the virus in liver, spleen, lung, trachea, and intestine samples. H&E staining revealed that hepatocytes were swollen and degenerated, and lungs showed interstitial pneumonia. Using IF, CIV mainly infected the lungs but not the liver, spleen, trachea, or intestines. From our analyses, the clinical symptom observation and

body temperature detection have the error of human factors, and the two can be used as the reference for the animal test of H3N2 subtype CIV infection. Severe lung consolidation occurred in 10^6 EID_{50}-infected dogs. Therefore, the degree of consolidation in lungs was an important criterion for the incidence of canine. Hence, our experiment lays a solid foundation for studying CIV pathogenesis and evaluating vaccine efficacy.

IAV pandemics are caused by novel viruses that efficiently sustain transmission into human populations with limited herd immunity. Dogs are potential mixing vessels for avian and mammalian IAVs and represent a human health concern due to their susceptibility to infection, their numbers, and close physical contact with humans [28]. It was reported that our isolates belonged to a distinct branch with mutations related to mammalian adaptation [29]. Our study provides increasing evidence that

Ge *et al. Virology Journal*   (2024) 21:151

Page 8 of 8

canine population surveillance for IAVs is an important component of pandemic preparedness.

Declarations

Ethics approval and consent to participate
The animal study protocols were approved by the Committee on the Ethics of Laboratory Animals of the Shanghai Animal Disease Control Center.

Consent for publication
The authors agree to publication.

Competing interests
The authors declare no competing interests.

References
1. Lee I-W, Kim Y-I, Lim G-J, et al. Comparison of the virulence and transmissibility of canine H3N2 influenza viruses and characterization of their canine adaptation factors. Emerg Microbes Infect. 2018;7(1):17. https://doi.org/10.1038/s41426-017-0013-x.
2. Crawford PC, Dubovi EJ, Castleman WL, et al. Transmission of equine influenza virus to dogs. Science. 2005;310(5747):482–5. https://doi.org/10.1126/science.1117950.
3. Lin D, Sun S. Natural and experimental infection of dogs with pandemic H1N1/2009 infuenza virus. J Gen Virol. 2012;93(Pt 1):119–23. https://doi.org/10.1099/vir.0.037358-0.
4. Song D, Kang B, Lee C, Jung K, et al. Transmission of avian infuenza virus (H3N2) to dogs. Emerg Infect Dis. 2008;14(5):741–6. https://doi.org/10.3201/eid1405.071471.
5. Sunchai Payungporn P, Cynda Crawford, Theodore S, Kouo, et al. Infuenza A virus (H3N8) in dogs with respiratory disease. Fla Emerg Infect Dis. 2008;14(6):902–8. https://doi.org/10.3201/eid1406.071270.
6. Li S, Shi Z. WanAvian-origin H3N2 canine infuenza a viruses in Southern China. Infect Genet Evol. 2010;10(8):1286–8. https://doi.org/10.1016/j.meegid.2010.08.010. Epub 2010 Aug 21.
7. Lee Y-N, Lee D-H, Park J-K, et al. Experimental infection and natural contact exposure of ferrets with canine infuenza virus (H3N2). J Gen Virol. 2013;94(Pt 2):293–7. https://doi.org/10.1099/vir.0.042473-0.
8. Lyoo K-S, Kim J-K, Kang B, et al. Comparative analysis of virulence of a novel, avian-origin H3N2 canine infuenza virus in various host species. Virus Res 2015 Jan. Epub 2014;2:195135–40. https://doi.org/10.1016/j.virusres.2014.08.020.
9. Jeoung H-Y, Lim S-I, et al. A novel canine infuenza H3N2 virus isolated from cats in an animal shelter. Vet Microbiol. 2013;165(3–4):281–6. https://doi.org/10.1016/j.vetmic.2013.03.021. Epub 2013 Apr 6.
10. Song DS, An DJ, Moon HJ, et al. Interspecies transmission of the canine influenza H3N2 virus to domestic cats in South Korea. J Gen Virol. 2011;92(Pt 10):2350–5. https://doi.org/10.1099/vir.0.033522-0. Epub 2011 Jun 29.
11. Zeng XJ, Lin Y, Zhao YB, et al. Experimental infection of dogs with H3N2 canine influenza virus from China. Epidemiol Infect. 2013;141(12):2595–603. Epub 2013 Mar 19.
12. Song D, Lee C, Kang B, et al. Experimental infection of dogs with avian-origin canine influenza a virus (H3N2). Emerg Infect Dis. 2009;15(1):56–8. https://doi.org/10.3201/eid1501.080755.
13. Chen Y, Zhong G, Wang G et al. Dogs are highly susceptible to H5N1 avian influenza virus.Virology, 2010,405(1):15–9. doi: 10.1016/j.virol.2010.05.024. Epub 2010 Jun 30.
14. Jung K, Lee CS, Kang BK, et al. Pathology in dogs with experimental canine H3N2 influenza virus infection. Res Vet Sci. 2010;88(3):523–7. Epub 2009 Dec 5.
15. Rogier Bodewes, Joost HCM, Kreijtz G, van Amerongen, et al. Infection of the upper respiratory tract with seasonal influenza A(H3N2) virus induces protective immunity in ferrets against infection with A(H1N1)pdm09 virus after intranasal, but not intratracheal, inoculation. J Virol. 2013;87(8):4293–301. https://doi.org/10.1128/JVI.02536-12. Epub 2013 Jan 30.
16. Minki H, Kang B, Na W, et al. Prolonged shedding of the canine influenza H3N2 virus in nasal swabs of experimentally immunocompromised dogs. Clin Exp Vaccine Res. 2013;2(1):66–8. https://doi.org/10.7774/cevr.2013.2.1.66. Epub 2013 Jan 15.
17. Shuo Su J, Tian M. eCollection Hong, Global and quantitative proteomic analysis of dogs infected by avian-like H3N2 canine influenza virus. Front Microbiol. 2015 Apr 2:6:228https://doi.org/10.3389/fmicb.2015.00228. 2015.
18. Lyoo K-S, Na W, Yeom M, et al. Virulence of a novel reassortant canine H3N2 influenza virus in ferret, dog and mouse models. Arch Virol. 2016;161(7):1915–23. https://doi.org/10.1007/s00705-016-2868-x. Epub 2016 Apr 30.
19. Tamura K, Nei M. Estimation of the number of nucleotide substitutions in the control region of mitochondrial DNA in humans and chimpanzees. Mol Biol Evol. 1993;10(3):512–26. https://doi.org/10.1093/oxfordjournals.molbev.
20. Tamura K, Stecher G, Peterson D, et al. MEGA6: molecular evolutionary genetics analysis version 6.0. Mol Biol Evol. 2013;30(12):2725–9. https://doi.org/10.1093/molbev. Epub 2013 Oct 16.
21. Luo J, Lu G, Ye S et al. Comparative pathogenesis of H3N2 canine influenza virus in beagle dogs challenged by intranasal and intratracheal inoculation. Virus Res 2018 Aug 15:255:147–53. https://doi.org/10.1016/j.virusres.2018.05.023. Epub 2018 May 31.
22. Jirjis FF, Deshpande MS, Tubbs AL, et al. Transmission of canine influenza virus (H3N8) among susceptible dogs. Vet Microbiol. 2010;144(3–4):303–9. https://doi.org/10.1016/j.vetmic.2010.02.029. Epub 2010 Mar 3.
23. Chen M, Wang R, Pei Y, Zhang T, Lyu Y, McLaughlin J, Vemaraju SSM, Wang Z. Yipeng Sun and Ming Zhang. Surveillance and characterization of avian-origin H3N2 canine infuenza viruses in 2021 in China. One Health Adv. 2024;2:2. https://doi.org/10.1186/s44280-023-00034-8.
24. Hailiang S, Blackmon S, Yang G, et al. Zoonotic risk, pathogenesis, and transmission of avian-origin H3N2 canine influenza virus. J Virol. 2017;91(21):e00637–17. https://doi.org/10.1128/JVI.00637-17. Print 2017 Nov 1.
25. SONG D, KANG B, LEE C, JUNG K, HA G, KANG D, PARK S, PARK B, OH J. Transmission of avian infuenza virus (H3N2) to dogs. Emerg Infect Dis. 2008;14(5):741–6. https://doi.org/10.3201/eid1405.071471.
26. Yongbo Liu C, Fu S, Ye Y, Liang Z, Qi C, Yao Z, Wang J, Wang S, Cai S, Tang Y, Chen S, Li. The inactivated vaccine of reassortant H3N2 canine influenza virus based on internal gene cassette from PR8 is safe and effective. Veterinary Microbiol 2021 Mar. 2021;254:108997. 10.1016/ j.vetmic.
27. De Luna X, Hartshorn KL. Influenza casts a lung shadow. Am J Pathol. 2017;187(4):697–9. https://doi.org/10.1016/j.ajpath.2017.01.007. Epub 2017 Feb 21.
28. Chen M, Lyu Y, Wu F, Zhang Y, Li H, Wang R, Liu Y, Yang X, Zhou L, Zhang M, Tong Q, Sun H. Juan Pu, Jinhua Liu, and Yipeng Sun. Increased public health threat of avian-origin H3N2 influenza virus caused by its evolution in dogs. Elife. 2023;12:e83470. https://doi.org/10.7554/eLife.83470. Published 2023 Apr 6.
29. HaiXiao Shen FF, Ge, et al. Epidemiological survey and genetic evolution of H3N2 subtype influenza viruses from stray dogs in Shanghai. China Virus Genes. 2020;56(3):329–38. https://doi.org/10.1007/s11262-020-01748-2. Epub 2020 Feb 27.

Publisher's Note